

Article

Preparation and Electrocatalytic Characteristics of PdW/C Catalyst for Ethanol Oxidation

Qi Liu †, Mingshuang Liu †, Qiaoxia Li * and Qunjie Xu *

Shanghai Key Laboratory of Materials Protection and Advanced Materials in Electric Power, College of Environmental and Chemical Engineering, Shanghai University of Electric Power, Shanghai 200090, China; E-Mails: lcdxliuqi@126.com (Q.L.); mingshuang1986@126.com (M.L.)

† These authors contributed equally to this work.

* Authors to whom correspondence should be addressed; E-Mails: liqiaoxia@shiep.edu.cn (Q.L.); xuqunjie@shiep.edu.cn (Q.X.); Tel.: +86-21-35303242 (Q.L.); +86-21-35304734 (Q.X.); Fax: +86-21-35303544 (Q.L.); +86-21-35304734 (Q.X.).

Academic Editor: Minhua Shao

Received: 12 May 2015 / Accepted: 15 June 2015 / Published: 29 June 2015

Abstract: A series of PdW alloy supported on Vulcan XC-72 Carbon (PdW/C) with total 20 wt. % as electrocatalyst are prepared for ethanol oxidation by an ethylene glycol assisted method. Transmission electron microscopy (TEM) characterization shows that PdW nanoparticles with an average size of 3.6 nm are well dispersed on the surface of Vulcan XC-72 Carbon. It is found that the catalytic activity and stability of the PdW/C catalysts are strongly dependent on Pd/W ratios, an optimal Pd/W composition at 1/1 ratio revealed the highest catalytic activity toward ethanol oxidation, which is much better than commercial Pd/C catalysts.

Keywords: ethylene glycol; PdW/C; catalyst; ethanol oxidation

1. Introduction

Development of novel catalysts with high electrocatalytic activity for ethanol oxidation has received much attention because the electroactivity of anodic materials is one of the main factors influencing the practical application of direct ethanol fuel cells (DEFCs) [1,2]. Palladium (Pd), as one of

platinum(Pt) group elements, could hold high electro-oxidation catalytic activity and has larger abundance and lower price compared to Pt [3,4]. Pd catalyst does not exhibit electroactivity for ethanol electro-oxidation in acid solutions, while it displays high electroactivity for ethanol electro-oxidation in alkaline solutions, such as NaOH and KOH [5,6].

Recently, Pd nanoparticle has attracted much attention due to their distinguished advantages, such as significantly large surface areas and high stability [7]. The interest in Pd metals is not only for lowering the cost of catalysts, but also for improving the catalytic activities [8]. One method to promote the catalytic activity of Pd is alloyed with other metals, including Ag [9,10], Fe [11] and Sn [12,13]. Many binary or ternary composite catalysts involved in Pd have been developed to enhance the electroactivity of the Pd catalyst for ethanol oxidation [14,15], such as Pd–Ru [16], Pd–Ni–P [17], Pd–Co [18], Pd–Pt [19,20], Pd–Au [21], and so on.

So, the addition of a second metal with Pd, to enhance its activity for ethanol electro-oxidation, is effective approach, but the durability with time of such electrode needs further improvement [22]. It has been claimed that tungsten (W) oxide was a suitable promoter for noble metal catalyst, leading to a significant decrease in poisoning species (CO) [23,24]. The presence of W species is expected to assist in the electro-oxidation of poisonous reaction intermediates adsorbed on the active Pd sites [25,26].

In this work, PdW/C catalysts with different Pd/W ratios were successfully prepared by an ethylene glycol assisted method. The catalytic activity and stability of PdW/C catalysts towards ethanol oxidation reaction (EOR) in alkaline solution were examined. The electrochemical properties of PdW electrocatalysts were also probed to explore their potential applications in DEFCs.

2. Results and Discussion

2.1. TEM

Figure 1 shows a typical TEM image of the prepared PdW/C and Pd/C catalysts. The nanoparticle sizes of PdW/C catalyst were primarily distributed within the range of 2–6 nm. The average PdW nanoparticles size of PdW/C was approximately 3.6 nm, whereas Pd nanoparticles of Pd/C were 5.2 nm. It should be pointed out that ethylene glycol as the reducing agent and dispersing agent, could effectively disperse the Pd nanoparticles. At the same time, the PdW nanoparticles size of PdW/C is smaller than Pd nanoparticles of Pd/C, indicating that demonstrating PdW/C is more beneficial for ethanol electro-oxidation in alkaline medium [27,28]. As shown in Figure 1, PdW/C catalyst was spherical and homogeneously dispersed on Vulcan XC-72 Carbon with no remarkable observation of agglomerations compared with Pd/C. High Resolution Transmission Electron Microscopy (HRTEM) image clearly shows the lattice fringe image of (1 1 1) planes with the interplanar distance of 0.2 nm. In Figure 1d, EDS of PdW/C shows the existence of Pd, W and C elements, illustrating the formation of W metal in as-obtained materials.

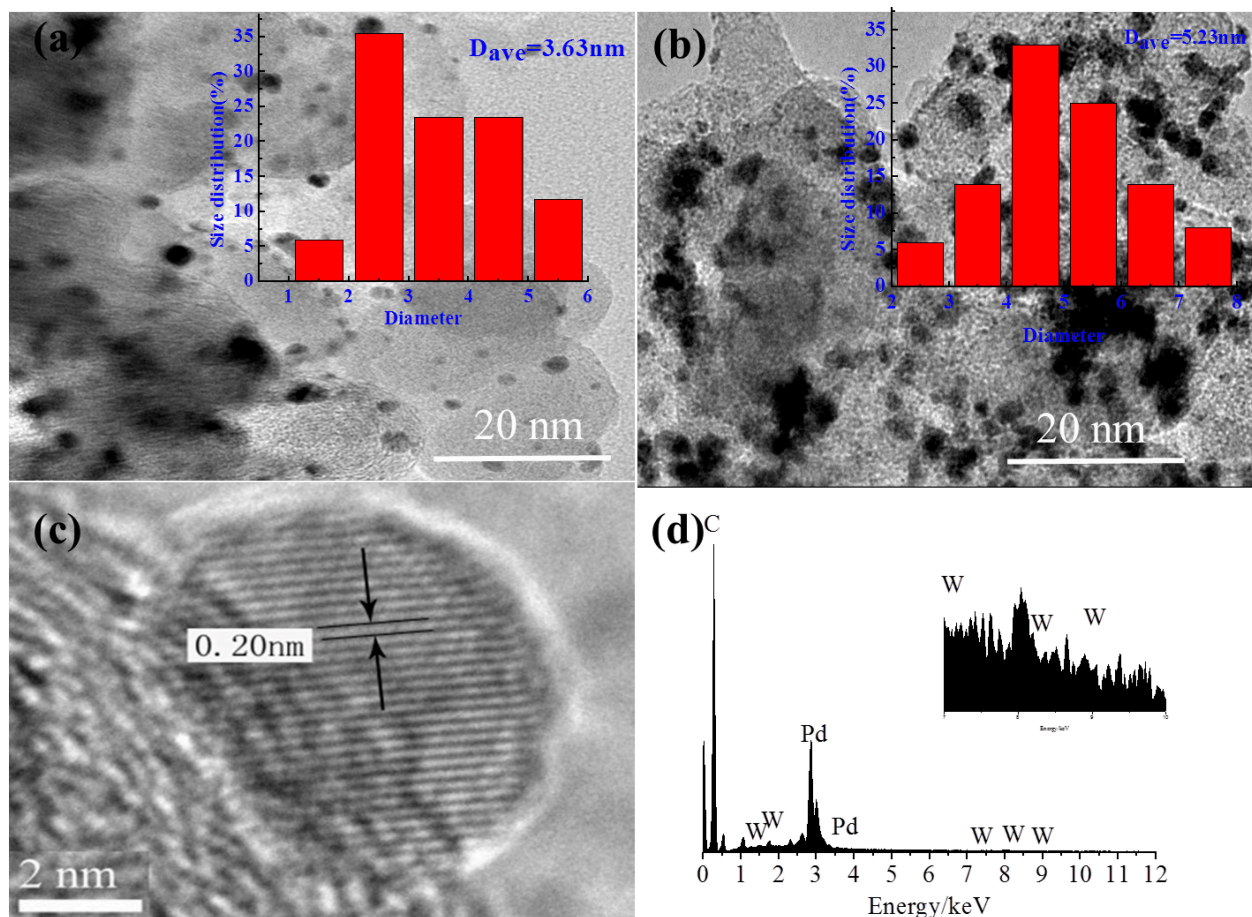


Figure 1. TEM images and their corresponding particle size distribution histograms (a) PdW/C; (b) Pd/C catalyst, respectively. (c) HRTEM images of PdW/C catalyst. (d) EDS of PdW/C catalyst.

2.2. XRD

The XRD patterns of W/C, Pd/C and PdW/C catalysts were shown in Figure 2. The typical diffraction peaks of WC around $2\theta = 26^\circ$ and 43° , is attributed to the C (002) and C (004), which are not W typical diffraction, as shown in the XRD patterns of Pd/C and PdW/C, and meanwhile C diffraction peaks also appeared. Sharp and well-defined peaks of Pd/C was observed at 2θ values of 40.14° , 46.69° , 68.17° , 82.17° , and 86.69° , corresponding to the planes of (1 1 1), (2 0 0), (2 2 0), (3 1 1), and (2 2 2), respectively, according to JCPDS No.65-6174. The strong diffraction peak of PdW/C catalyst was also found at 40.14° , corresponding to the plane of (1 1 1). No significant peak shift is observed for the PdW/C (1:1) [29]. The average particle size of the prepared PdW/C nanoparticles (d) was estimated by using the Scherrer Equation [30] after background subtraction from Pd (1 1 1) peak at 2θ of 40° , agreeing with TEM results, which is as shown in Table 1.

$$d = \frac{k\lambda}{\beta \cos \theta} \quad (1)$$

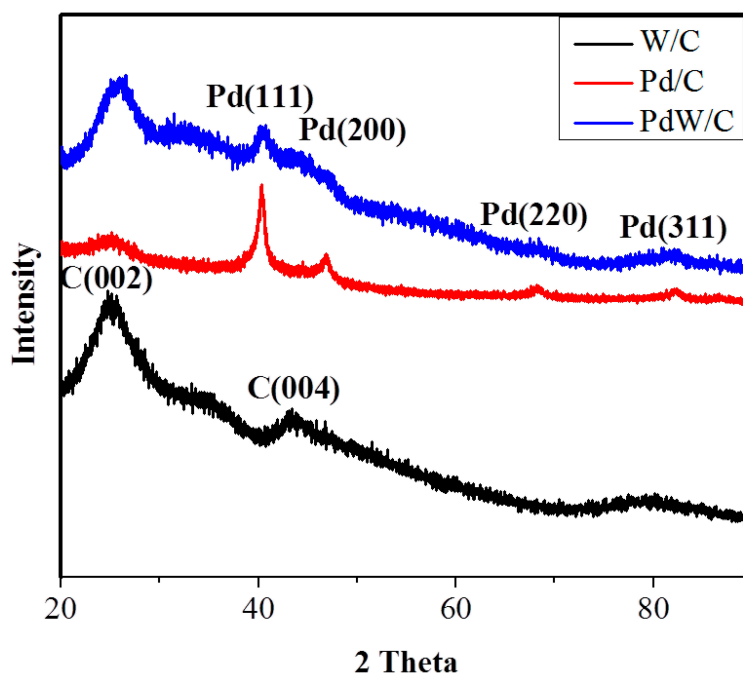


Figure 2. XRD patterns of PdW/C (1:1) and Pd/C.

Table 1. Summary of physical properties of PdW/C and Pd/C catalyst.

Catalysts	Pd Metal Loading Detected by ICP-AES	Diameter Calculated Form XRD/nm	Diameter Measured by TEM/nm	EASA/m ² ·g ⁻¹
PdW/C	10.6%	3.9	3.6	144.1
Pd/C	19.3%	5.74	5.32	71.2

2.3. Electrochemical Measurements

The cyclic voltammetry of PdW/C (1:1) and Pd/C in the absence of ethanol is shown in Figure 3. It is noted that they all exhibit significantly high anodic and cathodic current densities. The oxidation peak at lower anodic potential during the forward scan is ascribed to the formation of the adsorbed hydroxyl OH_{ads} while the peaks at high positive potential are related to the formation of Pd oxides [31,32]. The potential region from -1.1 to -0.6 V *versus* SCE on the CV curve of the catalyst is associated with the hydrogen adsorption/desorption. The potential region from -0.3 V to 0.3 V can be attributed to the formation of the palladium oxide layer on the surface of the PdW/C catalyst, and OH⁻ ions are first chemisorbed in the initial stage of the oxide formation at higher potentials, which are transformed into higher valence oxides. The electrochemical active surface areas (EASA) of PdW/C (1:1) and Pd/C was calculated to be 144.1 and 71.2 m²·g⁻¹, respectively (Table 2), indicating that PdW/C (1:1) has a higher electrochemical activity [33].

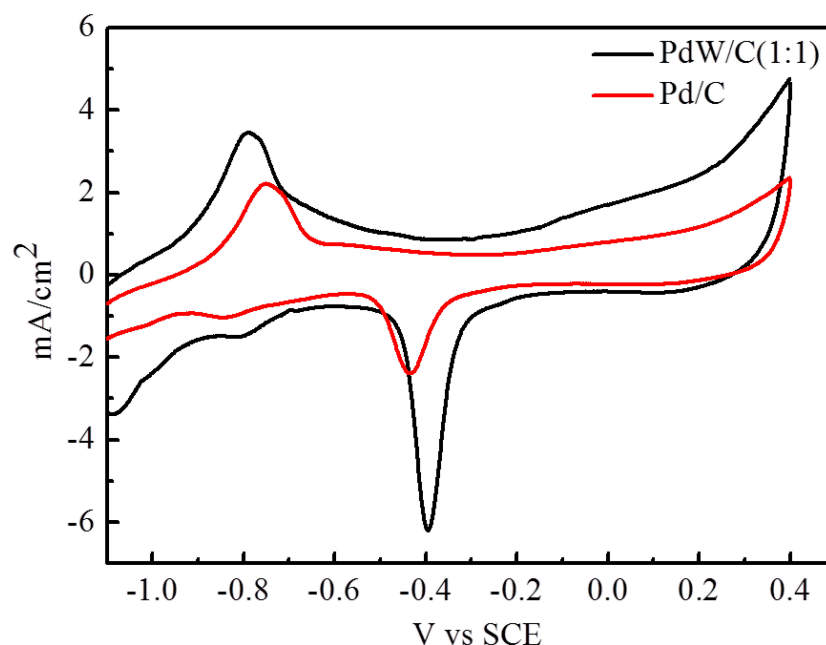
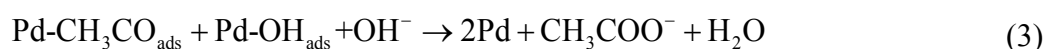
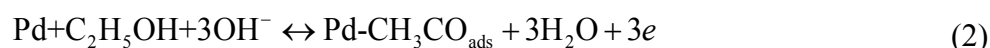


Figure 3. Voltammetric curves of PdW/C (1:1) and Pd/C in 1 M KOH solution at 50 mV·s⁻¹.

Table 2. Comparison of electrochemical performances on the prepared Pd-based catalysts.

Catalysts	$E_{\text{onset}}/\text{V}$	E_p/V	$i_p/\text{mA}\cdot\text{cm}^{-2}$	i (after 3600 s)/ $\text{mA}\cdot\text{cm}^{-2}$
PdW/C (1:1)	-0.71	-0.27	62.29	6.94
PdW/C (1:2)	-0.63	-0.32	14.02	0.42
PdW/C (2:1)	-0.68	-0.29	37.39	0.19
PdW/C (4:1)	-0.70	-0.40	15.37	0.03
Pd/C	-0.64	-0.25	39.58	1.58
Pd/C (JM)	-0.65	-0.17	48.70	2.29

Cyclic voltammetry was used to quantify the electrocatalytic activities of the Pd-based catalysts prepared at room temperature. Figure 4 shows the CV results detected in 1 M KOH + 1 M C₂H₅OH solution. The scan rate was selected at 50 mV·s⁻¹ in the potential range from -0.8 to 0.4 V. The oxidation peak in the forward scan corresponds to the oxidation of freshly chemisorbed species from ethanol adsorption. At a higher potential, the formation of PdO will block further adsorption of reactive species and lead to a remarkable decrease in current. During the negative-going sweep, the previously formed PdO will be reduced to catalytic active Pd, leading to the recovery of EOR current. Corresponding reactions are shown in Equations (2) and (3) [34]:



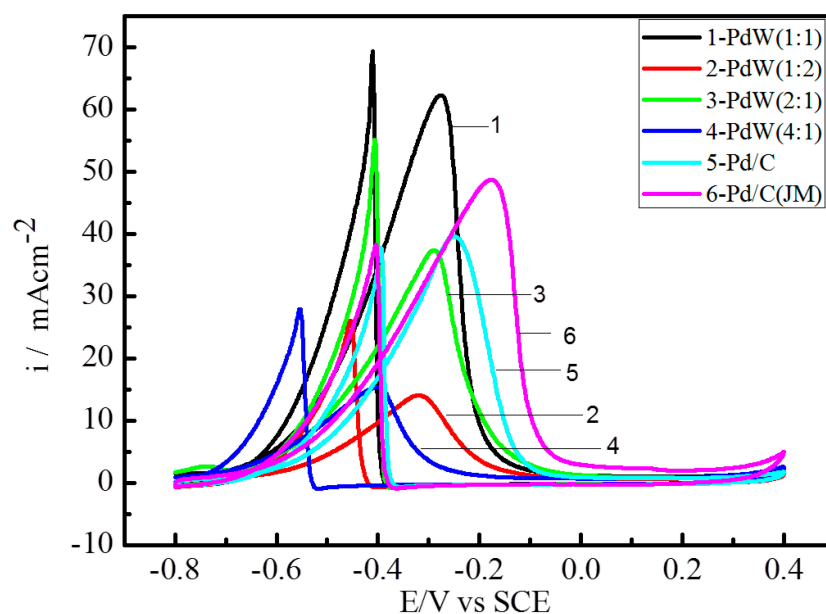


Figure 4. Voltammetric curves of Pd-based catalysts in 1 M KOH + 1 M C₂H₅OH solution at 50 mV·s⁻¹.

It is observed that the peak current density on PdW/C (1:1) is higher than those on other Pd-based catalysts (Figure 4), which could indicate that PdW/C (1:1) catalyst has the highest catalytic activity toward ethanol. In the forward scan, the onset potential (E_{onset}) of PdW/C (1:1) is -0.71 V, which has a negative shift of ~60 mV compared to that of Pd/C (JM) (-0.65 V). The peak current densities are 62.29 and 48.70 mA·cm⁻² (the area is the surface area of the electrode) for PdW/C (1:1) and Pd/C (JM), respectively, while their peak potentials are -0.27 and -0.17 V. The parameters, including the onset potential, the forward peak potential (E_p) and the forward peak current intensity (i_p) are shown in Table 2.

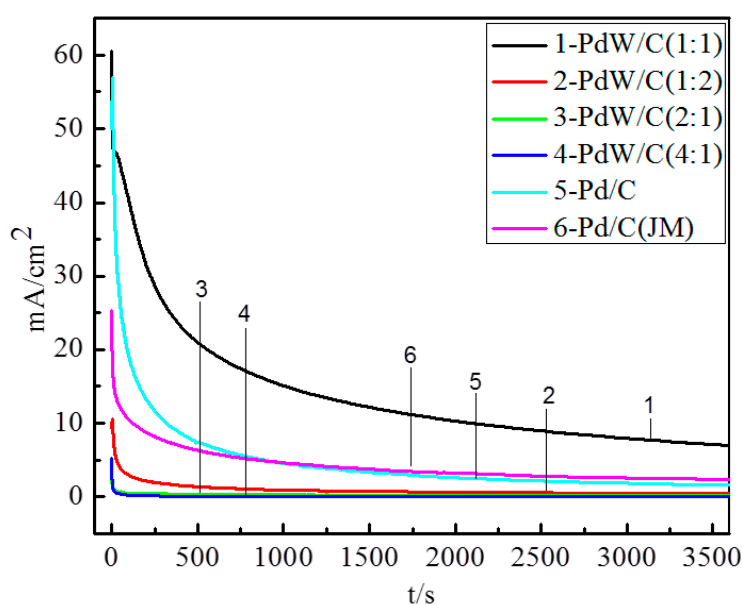


Figure 5. Chronoamperometry curves of Pd-based catalysts in 1 M KOH + 1 M C₂H₅OH solution at a fixed potential of -0.3 V at 50 mV s⁻¹.

Chronoamperometry was employed to evaluate the stability of the Pd-based catalysts. As shown in Figure 5, the current densities represent less decay at the applied constant potentials for 3600 s. The current density of ethanol electro-oxidation on the PdW/C (1:1) catalyst is $6.94 \text{ mA}\cdot\text{cm}^{-2}$, which is the highest among all the Pd-based catalysts, indicating that the PdW/C (1:1) exhibits a more stable electrocatalytic activity towards ethanol oxidation in the alkaline media than other catalysts. These results are in good accordance with the CV results.

3. Experimental Section

3.1. Materials

PdCl_2 was purchased from Shanghai Institute of Fine Chemical Materials (Shanghai, China); Vulcan XC-72 Carbon was supplied by Cabot Co. Ltd. (Boston, MA, USA); Tungsten hexachloride (99.5%, WCl_6), Ethylene glycol (AR, $\text{C}_2\text{H}_6\text{O}_2$), Sodium hydroxide (AR, Nelectro-oxidation H) and ethanol were obtained from Sinopharm Chemical Reagent Co. Ltd. (Shanghai, China) 5% Nafion[®] solution was provided by DuPont Co. Ltd (Wilmington, DE, USA); All reagents were of analytical reagent grade and used without further purification. The water utilized in the studies was double-distilled and deionized.

3.2. Catalyst Preparation

Vulcan XC-72 Carbon was treated in 5 M HNO_3 solution with vigorous stirring. A certain amounts with different ratios of WCl_6 and PdCl_2 were dissolved in 50 mL ethylene glycol. Subsequently, the pH of the solution was adjusted to 9 using 1 M NaOH solution. The mixtures were stirred for 1 h at 80 °C. The prepared carbon ethylene glycol solution was added in the mixture. After stirred for 3 h, the mixtures were filtered and washed several times with deionized water. The remaining solids were dried in a vacuum oven for 24 h at 80 °C. The weight percentages of metal were 20% in all catalysts. 20% Pd/C was prepared by the similar method. 20% commercial Pd/C (JM) catalyst was purchased from Johnson Matthet Company (Shanghai, China).

3.3. Characterization

XRD patterns were collected using a Bruker D8-Advance Powder X-ray diffractometer (Cu KR radiation, wavelength 1.5418 Å, Bruker, Germany). Transmission electron microscopy (TEM) images were characterized with a JEM-2100F HR-TEM model (JEM, Tokyo, Japan) using an accelerating voltage of 80 and 200 KV. 10.0 mg catalyst was dissolved in aqua regia (a strong acid mixture with HCl: HNO_3 volume ratio of 3:1) to form a Pd aqueous solution, and ICP-AES (Varian, Anaheim, CA, USA) was performed to detect the catalyst metal loading. All electrochemical measurements were performed in a standard three-electrode cell using a CHI 660C Electrochemical Analyzer (Chenhua Company, Shanghai, China).

3.4. Electrochemical Test

Cyclic voltammetry (CV) and chronoamperometry measurements were collected in 1 M KOH + 1 M C₂H₅OH solution at a scan rate of 50 mV·s⁻¹. The working electrodes were prepared, dropping 4 μL of the catalyst onto glassy carbon electrode (GCE, 0.07 cm²). The ink was prepared by ultrasonically mixing 5 mg of electrocatalyst sample in a mixture of 1 mL of ethanol and 120 μL of 5% Nafion[®] solution. The counter electrode was Pt foils and the reference electrode was saturated calomel electrode (SCE). The CV tests were carried out in the potential range of -0.8 to 0.4 V. Before experiments, pure nitrogen gas (99.99%) was bubbled through the solution at least 30 min to remove the dissolved oxygen in the solution.

4. Conclusions

In summary, Vulcan XC-72 Carbon supported 20 wt. % PdW/C catalysts with different Pd/W ratios were prepared by an ethylene glycol method. Among them, PdW/C (1:1) catalysts have a small average diameter (3.6 nm) and large electrochemical surface areas (144.1 m²·g⁻¹). It could also exhibit a higher reactivity toward EOR in alkaline electrolyte, compared to other PdW/C electrocatalysts. The peak current densities of PdW/C (1:1) (62.29 mA·cm⁻²) is higher than that of Pd/C (JM) (48.70 mA·cm⁻²). PdW/C (1:1) also exhibits more stable electrocatalytic activity than Pd/C (JM) towards ethanol oxidation in the alkaline media.

Acknowledgments

The project was supported by the National Science Foundation of China (21473039) and Shanghai Science and Technology Committee (No. 14DZ2261000).

Author Contributions

Qi Liu and Mingshuang Liu commonly carried out the catalyst preparation, electrochemical test and draft the manuscript. Qiaoxia Li and Qunjie Xu participated in the design of the study and helped to modify the manuscript. All authors read and approved the final manuscript.

Conflicts of Interest

The authors declare no conflict of interest.

References

1. Cai, Z.-X.; Liu, C.-C.; Wu, G.-H.; Chen, X.-M.; Chen, X. Green synthesis of Pt-on-Pd bimetallic nanodendrites on graphene via *in situ* reduction, and their enhanced electrocatalytic activity for methanol oxidation. *Electrochim. Acta* **2014**, *127*, 377–383.
2. Liu, Q.; Xu, Q.J.; Fan, J.C.; Zhou, Y.; Wang, L.L. A Review of Graphene Supported Electrocatalysts for Direct Methanol Fuel Cells. *Adv. Mater. Res.* **2015**, *1070–1072*, 492–496.
3. Li, Q.X.; Liu, M.S.; Xu, Q.J.; Mao, H.M. Preparation and Electrocatalytic Characteristics Research of Pd/C Catalyst for Direct Ethanol Fuel Cell. *J. Chem.* **2013**, *2013*, 1–6.

4. Ahmed, M.S.; Jeon, S. Highly Active Graphene-Supported Ni_xPd_{100-x} Binary Alloyed Catalysts for Electro-Oxidation of Ethanol in an Alkaline Media. *ACS Catal.* **2014**, *4*, 1830–1837.
5. Wang, Y.; Shi, F.-F.; Yang, Y.-Y.; Cai, W.-B. Carbon supported Pd–Ni–P nanoalloy as an efficient catalyst for ethanol electro-oxidation in alkaline media. *J. Power Sources* **2013**, *243*, 369–373.
6. Liang, Z.X.; Zhao, T.S.; Xu, J.B.; Zhu, L.D. Mechanism study of the ethanol oxidation reaction on palladium in alkaline media. *Electrochim. Acta* **2009**, *54*, 2203–2208.
7. Feng, L.; Zhang, J.; Cai, W.; Liang, L.; Xing, W.; Liu, C. Single passive direct methanol fuel cell supplied with pure methanol. *J. Power Sources* **2011**, *196*, 2750–2753.
8. Wang, Y.; He, Q.; Guo, J.; Wei, H.; Ding, K.; Lin, H.; Bhana, S.; Huang, X.; Luo, Z.; Shen, T.D.; *et al.* Carboxyl Multiwalled Carbon-Nanotube-Stabilized Palladium Nanocatalysts toward Improved Methanol Oxidation Reaction. *ChemElectroChem* **2015**, *2*, 559–570.
9. Lim, E.J.; Choi, S.M.; Seo, M.H.; Kim, Y.; Lee, S.; Kim, W.B. Highly dispersed Ag nanoparticles on nanosheets of reduced graphene oxide for oxygen reduction reaction in alkaline media. *Electrochem. Commun.* **2013**, *28*, 100–103.
10. Oliveira, M.C.; Rego, R.; Fernandes, L.S.; Tavares, P.B. Evaluation of the catalytic activity of Pd–Ag alloys on ethanol oxidation and oxygen reduction reactions in alkaline medium. *J. Power Sources* **2011**, *196*, 6092–6098.
11. Guo, S.; Sun, S. FePt nanoparticles assembled on graphene as enhanced catalyst for oxygen reduction reaction. *J. Am. Chem. Soc.* **2012**, *134*, 2492–2495.
12. Kim, J.; Momma, T.; Osaka, T. Cell performance of Pd–Sn catalyst in passive direct methanol alkaline fuel cell using anion exchange membrane. *J. Power Sources* **2009**, *189*, 999–1002.
13. Mao, H.; Wang, L.; Zhu, P.; Xu, Q.; Li, Q. Carbon-supported PdSn–SnO₂ catalyst for ethanol electro-oxidation in alkaline media. *Int. J. Hydrogen Energy* **2014**, *39*, 17583–17588.
14. Ding, K.; Wang, Y.; Yang, H.; Zheng, C.; Cao, Y.; Wei, H.; Wang, Y.; Guo, Z. Electrocatalytic activity of multi-walled carbon nanotubes-supported Pt_xPd_y catalysts prepared by a pyrolysis process toward ethanol oxidation reaction. *Electrochim. Acta* **2013**, *100*, 147–156.
15. Jiang, K.; Cai, W.-B. Carbon supported Pd–Pt–Cu nanocatalysts for formic acid electrooxidation: Synthetic screening and componential functions. *App. Catal.* **2014**, *147*, 185–192.
16. Sieben, J.M.; Comignani, V.; Alvarez, A.E.; Duarte, M.M.E. Synthesis and characterization of Cu core Pt–Ru shell nanoparticles for the electro-oxidation of alcohols. *Int. J. Hydrogen Energy* **2014**, *39*, 8667–8674.
17. Ding, L.X.; Wang, A.L.; Li, G.R.; Liu, Z.Q.; Zhao, W.X.; Su, C.Y.; Tong, Y.X. Porous Pt–Ni–P composite nanotube arrays: Highly electroactive and durable catalysts for methanol electrooxidation. *J. Am. Chem. Soc.* **2012**, *134*, 5730–5733.
18. Wang, Y.; Zhao, Y.; Yin, J.; Liu, M.; Dong, Q.; Su, Y. Synthesis and electrocatalytic alcohol oxidation performance of Pd–Co bimetallic nanoparticles supported on graphene. *Int. J. Hydrogen Energy* **2014**, *39*, 1325–1335.
19. Kim, Y.; Noh, Y.; Lim, E.J.; Lee, S.; Choi, S.M.; Kim, W.B. Star-shaped Pd@Pt core-shell catalysts supported on reduced graphene oxide with superior electrocatalytic performance. *J. Mater. Chem. A* **2014**, *2*, 6976.

20. Zhang, Y.; Chang, G.; Shu, H.; Oyama, M.; Liu, X.; He, Y. Synthesis of Pt–Pd bimetallic nanoparticles anchored on graphene for highly active methanol electro-oxidation. *J. Power Sources* **2014**, *262*, 279–285.
21. Datta, J.; Dutta, A.; Mukherjee, S. The Beneficial Role of the Cometal Pd and Au in the Carbon-Supported PtPdAu Catalyst Toward Promoting Ethanol Oxidation Kinetics in Alkaline Fuel Cells: Temperature Effect and Reaction Mechanism. *J. Phys. Chem. C* **2011**, *115*, 15324–15334.
22. Feng, L.; Yan, L.; Cui, Z.; Liu, C.; Xing, W. High activity of Pd–WO₃/C catalyst as anodic catalyst for direct formic acid fuel cell. *J. Power Sources* **2011**, *196*, 2469–2474.
23. Wang, Z.-B.; Zuo, P.-J.; Yin, G.-P. Effect of W on activity of Pt–Ru/C catalyst for methanol electrooxidation in acidic medium. *J. Alloy. Compd.* **2009**, *479*, 395–400.
24. Mellinger, Z.J.; Kelly, T.G.; Chen, J.G. Pd-Modified Tungsten Carbide for Methanol Electro-oxidation: From Surface Science Studies to Electrochemical Evaluation. *ACS Catal.* **2012**, *2*, 751–758.
25. Moon, J.-S.; Lee, Y.-W.; Han, S.-B.; Park, K.-W. Pd nanoparticles on mesoporous tungsten carbide as a non-Pt electrocatalyst for methanol electrooxidation reaction in alkaline solution. *Int. J. Hydrogen Energy* **2014**, *39*, 7798–7804.
26. Lu, Y.; Jiang, Y.; Gao, X.; Wang, X.; Chen, W. Strongly coupled Pd nanotetrahedron/tungsten oxide nanosheet hybrids with enhanced catalytic activity and stability as oxygen reduction electrocatalysts. *J. Am. Chem. Soc.* **2014**, *136*, 11687–11697.
27. Fan, Y.; Zhao, Y.; Chen, D.; Wang, X.; Peng, X.; Tian, J. Synthesis of Pd nanoparticles supported on PDDA functionalized graphene for ethanol electro-oxidation. *Int. J. Hydrogen Energy* **2015**, *40*, 322–329.
28. Hong, W.; Fang, Y.; Wang, J.; Wang, E. One-step and rapid synthesis of porous Pd nanoparticles with superior catalytic activity toward ethanol/formic acid electrooxidation. *J. Power Sources* **2014**, *248*, 553–559.
29. Wang, Y.; He, Q.; Ding, K.; Wei, H.; Guo, J.; Wang, Q.; O'Connor, R.; Huang, X.; Luo, Z.; Shen, T.D.; *et al.* Multiwalled Carbon Nanotubes Compositated with Palladium Nanocatalysts for Highly Efficient Ethanol Oxidation. *J. Electrochem. Soc.* **2015**, *162*, F755–F763.
30. Monshi, A.; Foughi, M.R.; Monshi, M.R. Modified Scherrer Equation to Estimate More Accurately Nano-Crystallite Size Using XRD. *World J. Nano Sci. Eng.* **2012**, *2*, 154–160.
31. Zhang, Z.; Xin, L.; Sun, K.; Li, W. Pd–Ni electrocatalysts for efficient ethanol oxidation reaction in alkaline electrolyte. *Int. J. Hydrogen Energy* **2011**, *36*, 12686–12697.
32. Maghsodi, A.; Milani Hoseini, M.R.; Dehghani Mobarakeh, M.; Kheirmand, M.; Samiee, L.; Shoghi, F.; Kameli, M. Exploration of bimetallic Pt-Pd/C nanoparticles as an electrocatalyst for oxygen reduction reaction. *Appl. Surf. Sci.* **2011**, *257*, 6353–6357.
33. Shi, J.; Ci, P.; Wang, F.; Peng, H.; Yang, P.; Wang, L.; Wang, Q.; Chu, P.K. Pd/Ni/Si-microchannel-plate-based amperometric sensor for ethanol detection. *Electrochim. Acta* **2011**, *56*, 4197–4202.

34. Yi, Q.; Niu, F.; Sun, L. Fabrication of novel porous Pd particles and their electroactivity towards ethanol oxidation in alkaline media. *Fuel* **2011**, *90*, 2617–2623.

© 2015 by the authors; licensee MDPI, Basel, Switzerland. This article is an open access article distributed under the terms and conditions of the Creative Commons Attribution license (<http://creativecommons.org/licenses/by/4.0/>).